EARTH SURFACE PROCESSES AND LANDFORMS
Earth Surf. Process. Landforms **35**, 1854–1866 (2010)

Published online 15 October 2010 in Wiley Online Library
(wileyonlinelibrary.com) DOI: 10.1002/esp.2074

Modelling the effect of time-dependent river dune evolution on bed roughness and stage

Andries J. Paarlberg,[1,2]* C. Marjolein Dohmen-Janssen,[2] Suzanne J. M. H. Hulscher,[2] Paul Termes[1] and Ralph Schielen[2,3]
[1] HKV Consultants, Lelystad, The Netherlands
[2] University of Twente, Enschede, The Netherlands
[3] Rijkswaterstaat Centre for Water Management (Waterdienst), Lelystad, The Netherlands

Received 7 December 2008; Revised 6 July 2010; Accepted 12 July 2010

*Correspondence to: Andries Jan Paarlberg, HKV Consultants, PO. Box 2120, 8203 AC, Lelystad, The Netherlands. E-mail: andries.paarlberg@hotmail.com

ESPL
Earth Surface Processes and Landforms

ABSTRACT: This paper presents an approach to incorporate time-dependent dune evolution in the determination of bed roughness coefficients applied in hydraulic models. Dune roughness is calculated by using the process-based dune evolution model of Paarlberg *et al*. (2009) and the empirical dune roughness predictor of Van Rijn (1984). The approach is illustrated by applying it to a river of simple geometry in the 1-D hydraulic model SOBEK for two different flood wave shapes. Calculated dune heights clearly show a dependency on rate of change in discharge with time: dunes grow to larger heights for a flood wave with a smaller rate of change. Bed roughness coefficients computed using the new approach can be up to 10% higher than roughness coefficients based on calibration, with the largest differences at low flows. As a result of this larger bed roughness, computed water depths can be up to 15% larger at low flow. The new approach helps to reduce uncertainties in bed roughness coefficients of flow models, especially for river systems with strong variations in discharge with time. Copyright © 2010 John Wiley & Sons, Ltd.

KEYWORDS: river dunes; hydraulic roughness; modelling

Introduction

Water levels computed by hydraulic simulation models are mainly controlled by flow resistance coefficients (e.g. Casas *et al*., 2006; Vidal *et al*., 2007; Morvan *et al*., 2008). Various elements in a river system contribute to the flow resistance, such as groynes, bedforms, vegetation in floodplains or other elements obstructing the flow. Over the past decade, several elements in hydraulic models were improved (e.g. accuracy of bathymetry, cross-section schematization, characterization of floodplain vegetation). However, the roughness coefficients of the main channel and the floodplain still have large uncertainties and significantly influence water-level predictions (e.g. Van der Klis, 2003; Paarlberg, 2007; Warmink *et al*., 2007).

The flow resistance of the main channel is largely determined by form drag due to river dunes which is mainly controlled by the dune shape (i.e. dune height and length, or aspect ratio). Therefore, a range of relationships exists that link a roughness coefficient to dune geometry (e.g. Vanoni and Hwang, 1967; Yalin, 1972; Van Rijn, 1984; Karim, 1995). River dunes are found in nearly all fluvial river systems, with the river bed consisting of sand, gravel or mixtures (e.g. Kostaschuk, 2000; Wilbers and Ten Brinke, 2003; Best, 2005; Jerolmack and Mohrig, 2005; Kleinhans *et al*., 2007; Figure 1).

For steady flows a wide range of formulas is available to predict equilibrium dune dimensions as a function of a range of parameters such as flow strength, flow depth or sediment size (e.g. Yalin, 1964; Allen, 1968; Van Rijn, 1984; Julien and Klaassen, 1995; Coleman *et al*., 2005). For unsteady river flows dune dimensions generally depend on (1) the equilibrium dune dimensions for a specific set of flow conditions, (2) the actual dune dimensions and (3) the rate of change of discharge with time. This complicates the determination of bed roughness over the complete timescale of a flood wave. Figure 2b shows measured dune heights during the 1998 flood in the River Rhine near the Pannerdensche Kop (Figure 1) as a function of the discharge. A clear hysteresis in dune height is observed, which occurs because it requires time for the dunes to adapt to the changing flow conditions by means of sediment transport. After the discharge peak, the dunes continue to grow about 20% in height. Although we lack water-level measurements for this particular case, Figure 2a shows a significant hysteresis effect in water levels in the River Meuse in the Netherlands. This effect can be attributed to (i) accelerations and decelerations during the passage of a flood wave (the so-called Jones effect; see, for example, Jansen *et al*., 1979; Perumal *et al*., 2004) and (ii) time-dependent dune evolution and associated bed roughness during the passage of a flood wave.

Wilbers (2004) proposed a method to take unsteady flow conditions into account in bed roughness predictions, following the approach of Allen (1976). This approach requires the use of a calibrated adaptation constant, limiting the general applicability of the model. Giri *et al*. (2007) developed a morphodynamic simulation code which is able to predict stage–discharge relationships under flume conditions. However, the detailed and complicated flow model results in extremely large computational times and makes the model infeasible for operational water management purposes.

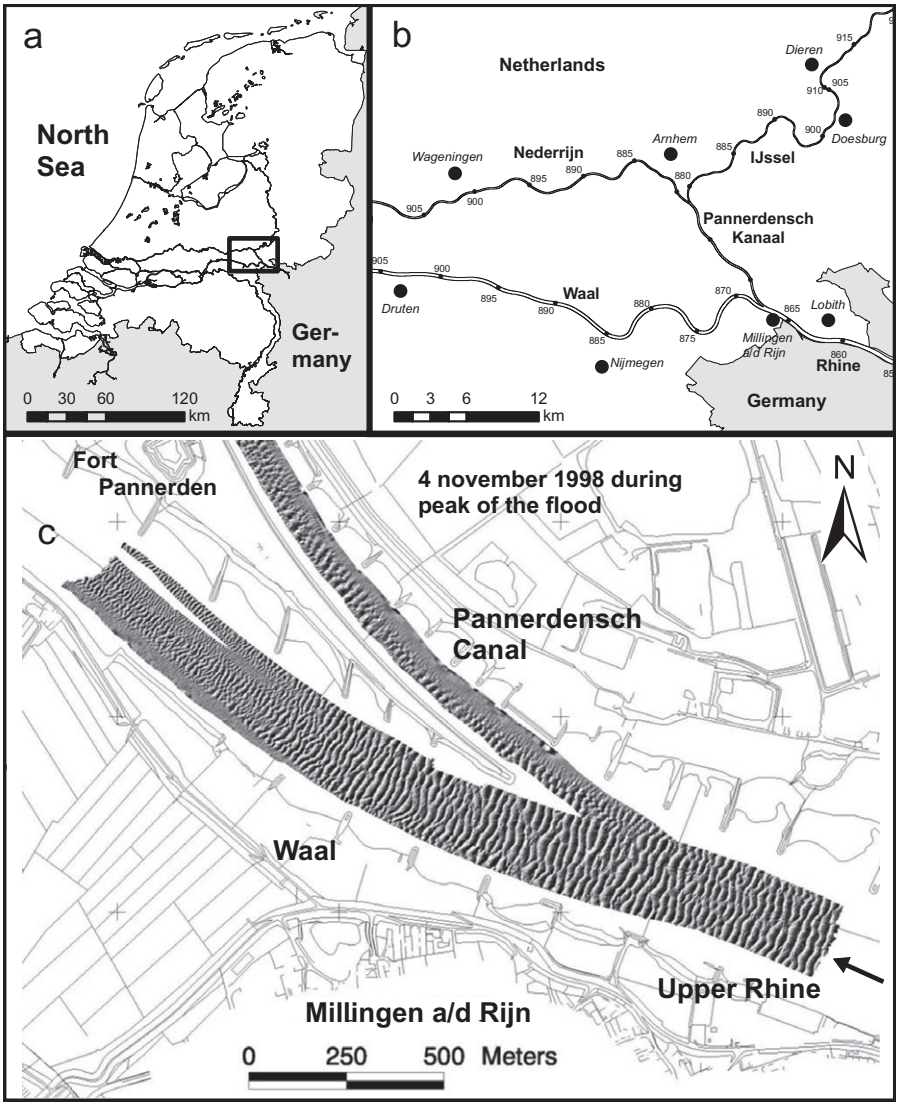

Figure 1. Measurements of dunes at the 'Pannerdensche Kop' river bifurcation in the Netherlands. (a) Location in the Netherlands. The River Rhine enters the Netherlands from the east and the River Meuse enters the Netherlands from the south. (b) Major river branches of the River Rhine. The numbers along the rivers are distance measurements in kilometres. (c) Multibeam measurements during the peak of a 1998 flood wave, with dune heights of 1–2 m and lengths of up to 50 m in an average water depth of about 10 m. (Picture courtesy of Antoine Wilbers ©.)

For practical reasons bed roughness coefficients of hydraulic models are often calibrated to match observed and computed water levels and discharge (distributions) (e.g. Wasantha Lal, 1995; Werner, 2004; Van den Brink *et al*., 2006). Often, a time-independent bed roughness is applied over the full timescale of a flood wave, meaning that only parts of a flood wave can be reproduced accurately. For a 1-D (SOBEK) model of the River Rhine in the Netherlands the main channel roughness coefficients were calibrated as a function of the discharge, to obtain better results for the complete timescale of flood waves (Udo *et al*., 2007). However, this still implies that there is one unique value for the roughness coefficient for every discharge. This means that the calibration is specific for the conditions (e.g. peak discharge, flood wave shape) for which the model was calibrated. In other words, the effects of time-dependent dune evolution and the evolution of bed roughness are incorporated into the calibrated roughness coefficient of the main channel.

This paper investigates (1) how bed roughness and water-level predictions differ if we use (a) calibrated *time-independent* or (b) calculated *time-dependent* roughness coefficients and (2) whether dune evolution and associated bed roughness vary significantly for different flood wave shapes. To this end, we have developed a dynamic roughness model by extending the 1-D hydraulic simulation model SOBEK with a model to predict time-dependent dune roughness. This dune roughness model consists of an idealized process-based dune evolution model (Paarlberg *et al*., 2009) and a roughness predictor, translating dune geometry into a bed roughness coefficient. Since the underlying dune evolution model is set up to minimize the required computational effort, the new simulation model can be applied at flood wave timescales.

In the next section the various submodels of the dynamic roughness model are explained. The case study that we use in this paper, a representative SOBEK schematization of the River Waal, is illustrated in the third section. In the same section, the two analysed flood wave shapes and the method to analyse the differences in water-level predictions between a model using (a) calibrated time-independent or (b) calculated time-dependent bed roughness coefficients are discussed. The model results are presented in the fourth section. First, we focus on simulated dune dynamics for both types of flood waves; then, we discuss the effects of including time-dependent dune roughness on water-level predictions. The paper ends with a discussion and conclusions, in the final two main sections.

Hydraulic Model Including Time-Dependent Dune Roughness

Dynamic roughness model

The dynamic roughness model presented in this paper extends the existing hydraulic simulation model SOBEK with two sub-

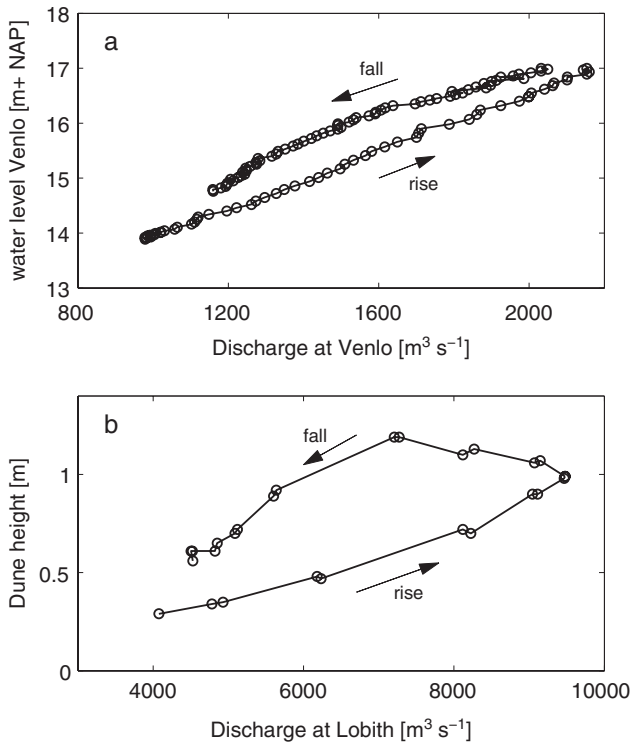

Figure 2. (a) Hysteresis in water level in the River Meuse at Venlo during the February 2002 flood (Termes, 2004). NAP is a Dutch ordinance datum. (b) Hysteresis in dune height in the River Rhine near the Pannerdensche Kop during a 1998 flood wave (data from Directorate Eastern Netherlands (DON) and the Head Office of Rijkswaterstaat; see also Wilbers and Ten Brinke, 2003).

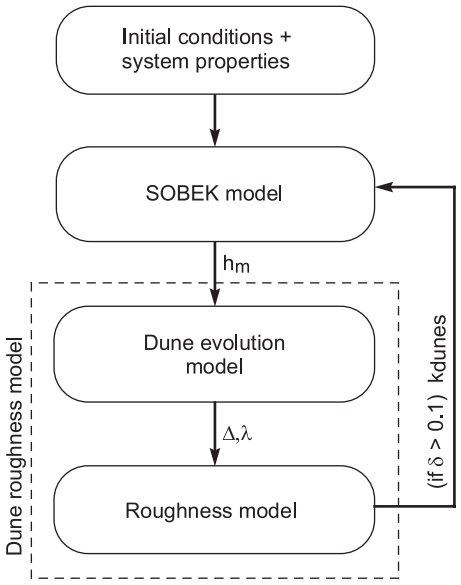

Figure 3. Overview of the dynamic roughness model presented in this paper, which consists of the existing hydraulic simulation model SOBEK and a dune roughness model. A simulation is initialized by specification of a discharge wave, system properties (such as grain size) and initial dune height. The water depth in the main channel (h_m) computed by SOBEK is used as input for the dune evolution model to compute dune height Δ and dune length λ. The roughness model translates these dune dimensions into a Nikuradse roughness height k_{dunes} . If the relative change in roughness height (δ) is larger than 10%, a new SOBEK computation is performed.

models to calculate time-dependent dune dimensions and associated bed roughness during flood waves (Figure 3). Dune dimensions are computed by solving an idealized morphodynamic model that runs separately from SOBEK, as discussed below. The dune evolution model uses the average water depth h_m as computed by SOBEK as input. Computed dune dimensions are translated into a Nikuradse roughness height by using an empirical roughness height model. For steady flow, a 10% change in roughness height results in a change of water depth of 1–2%. Therefore water levels are updated by SOBEK only if the relative change in roughness height during a simulation is 10% or more (Figure 3). The approach to determine the dune length in the dynamic roughness model is explained in the final subsection of this section.

Hydraulic model SOBEK

In the Netherlands, the hydraulic model SOBEK is used to make water-level predictions for the rivers Rhine and Meuse (Figure 1). SOBEK solves the 1-D cross-sectional integrated shallow-water equations. The river is divided into trajectories of a certain length, and cross-sections are defined roughly every 500 m, to take large-scale variations in bed levels and river non-uniformity in stream direction into account. The specific SOBEK schematization of the River Waal, which is used in this paper, along with required boundary conditions, will be discussed in the next main section.

Dune evolution model

Dune dimensions are calculated with the dune evolution model of Paarlberg *et al*. (2009), using the reach-averaged channel slope, the average water depth in the main channel (as computed by SOBEK) and the bed material (represented as D_{50}) as inputs. This morphodynamic simulation model is based on the two-dimensional vertical (2-DV) shallow-water equations with hydrostatic pressure assumption. As basic turbulence closure, a constant eddy viscosity over the water depth and a partial slip condition at the bed are employed. Two coefficients of the turbulence model which determine the values of the eddy viscosity and resistance at the bed were calibrated on the basis of flume experiments (see Paarlberg *et al*., 2009, for details) and in this paper the model is applied with the same calibrated coefficients (see also Paarlberg, 2008).

Flow separation is included in a parametrized way. In the region of flow separation, the separation streamline forms an artificial bed (Paarlberg *et al*., 2007), enabling computation of hydrostatic flow over the dunes. An empirical sediment transport relationship including gravitational bed slope effects is applied to determine bed evolution. In the flow separation zone, bed shear stresses and sediment transport rates are set to zero. Sediment passing the crest of a dune deposits on the lee face at the angle of repose.

Roughness model

In this paper we determine the roughness coefficient of the main channel as a Nikuradse roughness height. This roughness height is translated into a Chézy coefficient for use in SOBEK by using a Colebrook–White type formula (ASCE Task Force on Friction Factors in Open Channels, 1963; Van Rijn, 1984):

$$C_m = 18\log\left(\frac{12h_m}{k_m}\right) \quad (1)$$

in which C_m is the Chézy coefficient of the main channel, k_m is the Nikuradse roughness height of the main channel and h_m is

the average water depth in the main channel as computed by SOBEK. Following Van Rijn (1984), the roughness height of the main channel (k_m) can be divided into a contribution of grains (k_{grains}) and dunes (k_{dunes}):

$$k_m = k_{grains} + k_{dunes} \tag{2}$$

Generally, if dunes are present, form drag due to dunes is dominant over the grain roughness (e.g. Knighton, 1998; Julien *et al*., 2002; De Vriend, 2006). Grain roughness k_{grains} is specified as $3D_{90}$ (Van Rijn, 1993). Note that if the roughness coefficients of a hydraulic model are calibrated to reproduce measured water levels, all uncertainties and (model) errors end up in the calibrated roughness coefficient; this will be further examined in the Discussion of this paper. To close our model, we need a relationship between computed dune dimensions and roughness height k_{dunes}. Although numerous relationships are proposed in the literature, we chose to use the relationship of Van Rijn (1984). Van Rijn's relationship is based on an extensive database of both flume and field measurements, and is widely applied, particularly for field studies (e.g. Julien *et al*., 2002; Sieben, 2003). The empirical relationship of Van Rijn (1984, 1993) reads

$$k_{dunes} = 1{\cdot}1\gamma\Delta\left(1-\exp\frac{-25\Delta}{\lambda}\right) \tag{3}$$

in which Δ is the dune height and λ is the dune length. The shape factor γ expresses the influence of the dune shape on the roughness height. The shape factor γ is 1 for dunes with angle-of-repose slip faces, since Van Rijn (1984) based his relationship on such dunes. However, in the field, the dune lee slope is often less than the angle of repose (Ogink, 1988; Van Rijn, 1993; Van der Mark *et al*., 2007). As a result, flow separation might be less pronounced (or in some cases even absent), reducing the form drag due to dunes. Since our dune evolution model assumes an angle-of-repose leeside, it is considered that the roughness is overestimated for field conditions. Therefore, we apply a value of $\gamma = 0{\cdot}7$, as was proposed by Van Rijn (1993), based on field measurements of various river systems.

The dune evolution model used in this paper is 2-DV (see above) and thus explicitly assumes that dunes form uniformly over the complete main channel width, that all dunes have the same height, and that all available energy and bed load transport directly contribute to the formation of dunes. In reality, however, dunes might be of different size near the banks or part of the transported sediment passes the crest or is in suspension without contributing to dune formation. Therefore, it is anticipated that our dune evolution model predicts maximum dune dimensions in rivers rather than average dune dimensions. Van der Mark *et al*. (2007) analysed flume data and found that the average dune height is more or less half the maximum dune height. Calculated dune aspect ratios (Δ/λ) are more or less constant (see Results section), meaning that dune roughness linearly depends on dune height (Equation (3)). To use the average dune height, rather than the maximum dune height, in the prediction of bed roughness we chose to halve the dune shape factor, i.e. we use $\gamma = 0{\cdot}35$ as correction factor in Equation (3) to determine the Nikuradse roughness height. In the Discussion, the sensitivity of computed roughness coefficients and water levels to this parameter is investigated.

Method to determine dune length

In this paper we study dune dynamics and water levels in a uniform channel (see next section), which means that dunes will be distributed more or less uniformly over the river reach. Therefore, we simulate the dynamics of a single dune in a computational domain with periodic boundary conditions in the horizontal direction. It is assumed that this dune, and associated form drag and resistance coefficient, is representative for the whole river reach.

Wilbers and Ten Brinke (2003) observed that in the River Waal (near Druten) the dune length remains fairly constant during a flood, i.e. about 40 m. They argue that this is caused by a combination of grain size distribution over the river width and distance between groynes in the River Waal. However, for other river sections such as the Upper Rhine between Lobith and the Pannerdensche Kop (Figure 1), the dune length may vary during floods. More specifically, Wilbers and Ten Brinke (2003) observed that the dune length continues to grow, while the discharge is already falling after the discharge peak. Instead of decreasing dune lengths during the falling stage (during the falling stage of a flood, decreasing dunes lengths could be expected as a result of the decreasing water depth, since dune length primarily scales with the water depth), smaller secondary dunes form on the primary dunes at the end of a flood. This is related to the inability of the large primary dunes to diminish in length because this requires sediment transport, which decreases in magnitude because of decreasing flow strength during the falling stage of a flood wave.

To analyse the effects of a changing dune length on dune heights and water levels, simulations are performed using a constant and a variable dune length. Since we use periodic boundary conditions in the dune evolution model, the dune length does not automatically change. However, the dune length can be changed by changing the length of the domain. The dune length is determined by the simulation model on the basis of a numerical linear stability analysis (Dodd *et al*., 2003), and is mainly controlled by the water depth in our model. If the water depth changes by 1%, the simulation model performs a linear stability analysis using small-amplitude sinusoidal disturbances with different wavelengths on a flat bottom as topography (see also Paarlberg *et al*., 2009). Typically, a 1% change in water depth results in a 1% change in dune length. It is assumed that the dune length found from the linear analysis is a good representation of the dune length in the nonlinear regime as well (e.g. Dodd *et al*., 2003; Németh *et al*., 2006; Paarlberg *et al*., 2009).

An example result of the linear stability analysis is shown in Figure 4. From this analysis a fastest-growing wavelength is found and is used as domain length (effectuated by adapting the horizontal distance between grid points in a horizontal direction). Note that using this approach the dune length becomes smaller during the falling stage of a flood wave, since it mainly scales with the flow depth. This is not in agreement with the observed behaviour of the dune length of primary dunes in the River Waal outlined above. However, it may represent the smaller secondary dunes forming on top of these large primary dunes during the falling stage of a flood wave.

Model Setup and Methodology for Analysis

Representative River Waal schematization

The SOBEK Rhine model covers the non-tidal part of the Dutch Rhine branches. This model contains two river bifurcations (Figure 1b) and model results are sensitive to the discharge

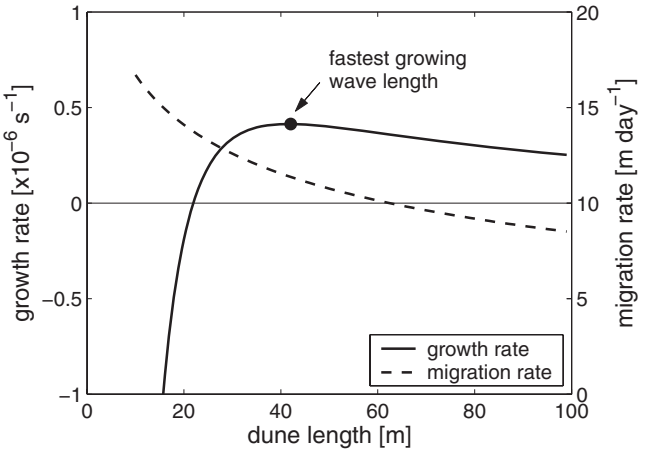

Figure 4. Results of a numerical linear stability analysis for a main channel water depth of 6 m. Dunes with a length shorter than 20 m shrink because of negative growth rates. In this example, a dune with a wavelength of ~40 m has the largest growth rate and is used as dune length in a simulation. The stability analysis is repeated if the water depth changes by 1% due to dune evolution.

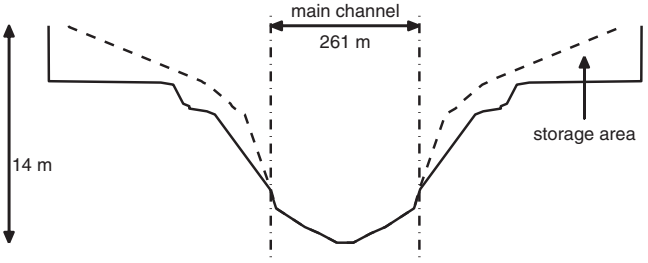

Figure 5. Cross-section for the SOBEK model, based on a relatively straight section in the River Waal (river km 895·34, Figure 1b). The solid line represents the actual bathymetry. The part of the cross-section which is below the dashed lines only stores water, for example, in deep pools in the floodplain (i.e. it does not contribute to the conveyance of the channel).

distribution at these bifurcations. To avoid such effects we set up a simple 60 km long straight channel with floodplains in SOBEK, having a uniform cross-section that is representative for a relatively straight trajectory in the River Waal (river km 885·23–900·88) (Figure 5).

Computed roughness coefficients are uniform over the entire reach and SOBEK computes the water level along the channel. At the downstream end of the model, a stage–discharge relationship is used. To minimize the influence of the downstream stage–discharge relationship on the results, the average flow depth (h_m) at the upstream boundary of the main channel is used as input for the dune evolution model (typically, the adaptation length scale of disturbance in the River Waal is some tens of kilometres). The grain size distribution and channel slope are uniform over the entire reach. Based on conditions in the River Waal we specify D_{50} as 1 mm and D_{90} as 10 mm (Wilbers and Ten Brinke, 2003; Kleinhans *et al.*, 2007) and the channel slope i as $0{\cdot}76 \times 10^{-4}$.

Flood wave scenarios

Flood waves in the River Rhine are variable in shape, with rapid or gradual changes in discharge over time (Figure 6). For some waves the flood wave has a sharp peak (high discharge for a short period of time), while other waves are characterized by a longer period of high discharge. The discharge in the River Waal is about 2/3 of that of the River Rhine at Lobith, because of the bifurcation at the Pannerdensche Kop (Figure 1).

Since we are interested in dune dynamics and the effects of dunes on water levels for different flood wave shapes, we analyse two different flood wave shapes, as presented in Figure 7. The sharp-peaked (SP) flood wave (Figure 7a) is based on the flood wave that occurred in the River Waal in October and November 1998, which had a maximum discharge of about 6000 m^3 s^{-1} in the River Waal. The wave is characterized by a sharp peak, i.e. the high discharge occurs for a small period of time. For the broad-peaked (BP) flood wave (Figure 7b) we chose the same maximum discharge, but this discharge occurs for a longer period of time such that the total duration of the two flood waves is equal (i.e. 30 days). These shape differences may influence dune dynamics, since for the broad-peaked wave (1) the rising and falling stages are shorter, implying a larger rate of change of discharge with time, and (2) the dunes have more time to adapt to the higher discharge since this lasts longer. This yields a relatively long period of high discharge for the broad-peaked flood wave (with a zero rate of change in discharge) in which the dunes evolve towards the equilibrium dune height. Although this broad-peaked flood wave shape is rather artificial the effect of variable rate of change can be investigated with these two flood wave shapes.

Generally, dune dimensions at the start of a flood wave are not known, but in the simulation model initial dune dimensions have to be specified. We have chosen to start a simulation with an initial dune height of 2 cm. A model simulation consists of a series of two flood waves of identical shape with a period of 1 week of constant low discharge in between (Figure 7). For the first wave (indicated by 'SP1' and 'BP1' in Figure 7), dunes have to develop from very small sinusoidal waves, while for the second wave (indicated by 'SP2' and 'BP2' in Figure 7), the dune height is more or less in equilibrium with flow conditions as the second wave starts.

Comparison of Sobek models with different roughness formulations

Hysteresis in water levels is caused by a combined effect of dune dynamics and accelerations and decelerations during the passage of a flood wave. In the SOBEK Rhine model of Udo *et al*. (2007), roughness coefficients for the main channel and floodplain are calibrated for a certain number of trajectories, as a function of the discharge. Thus for each discharge there is one unique value of the Chézy coefficient. The aim of the new extended SOBEK model is to analyse the effects of hysteresis in dune dimensions on water levels, for different flood wave shapes. Figure 8 illustrates the approach used to analyse the differences between a SOBEK model using computed and calibrated roughness coefficients.

The calibrated roughness coefficients are used to compare the results of the extended model with the original SOBEK model (Figure 8). Figure 9 shows the calibrated Chézy coefficients for the river trajectory on which our SOBEK model is based (Figure 5). For this calibration, recorded discharges (up to 7000 m^3 s^{-1} in the River Waal) and water levels of various flood waves were used. For discharges higher than about 7000 m^3 s^{-1}, the SOBEK model was calibrated on the basis of simulation results of the 2-DH hydraulic model WAQUA of the River Rhine in the Netherlands (Van den Brink *et al.*, 2006; Udo *et al.*, 2007). In this paper, we focus on discharges $\leq$6000 m^3 s^{-1} in the River Waal, since this is the recorded maximum discharge for the 1998 flood. Since the roughness of the floodplain is not of central interest in this paper, we base

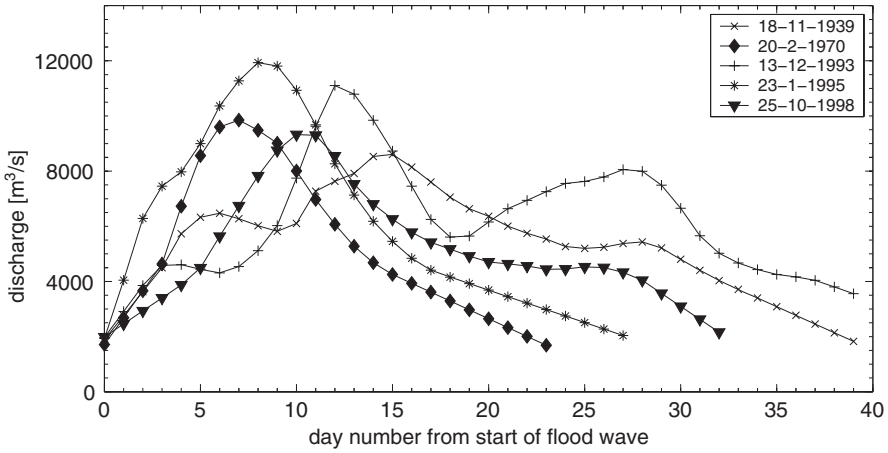

Figure 6. Some recorded flood waves in the River Rhine at Lobith, upstream of the first bifurcation in the Netherlands.

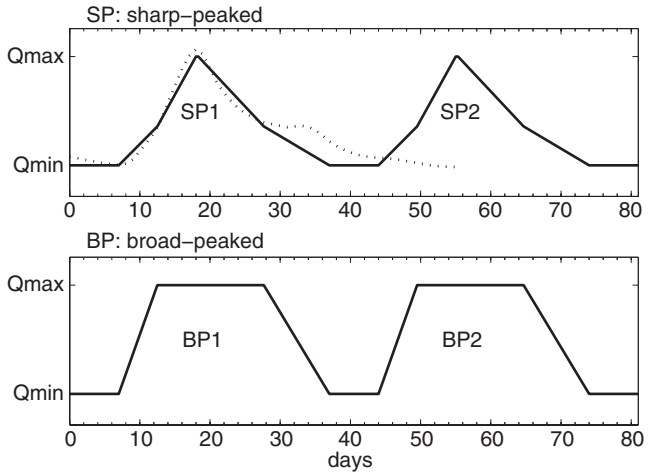

Figure 7. Two types of flood waves analysed in this paper. Qmax (= 6000 $m^3 s^{-1}$) and Qmin (= 1333 $m^3 s^{-1}$) are the maximum and minimum simulated discharges in the River Waal, respectively. The dotted line in the top plot gives the recorded hydrograph for the 1998 flood in the River Waal. In the simulations, a series of two waves of identical shape are simulated, for which the numbering is indicated in the plots ('SP' is sharp-peaked and 'BP' is broad-peaked). Note that the waves are not symmetrical, with longer falling stages than rising stages, in line with observed flood waves (Figure 6).

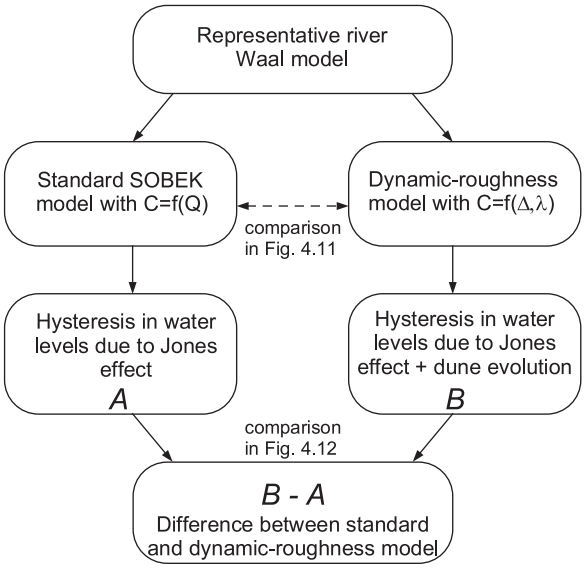

Figure 8. Illustration of the approach to analysing differences between a SOBEK model using calibrated (*A*) and computed (*B*) roughness coefficients. C is the Chézy coefficient and Q is the river discharge.

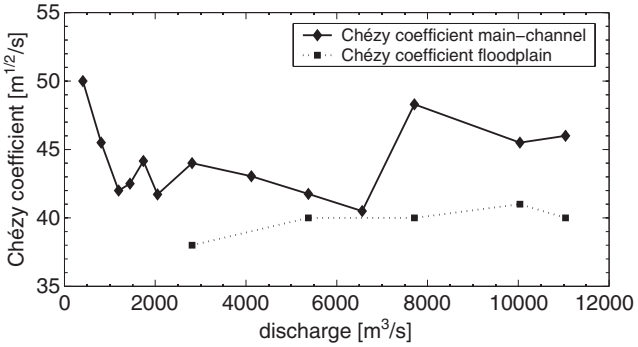

Figure 9. Calibrated Chézy coefficients of the main channel and the floodplain as a function of discharge in the Waal for trajectory with river km 885·23–900·88 (data from Udo *et al.*, 2007).

the roughness coefficient of the floodplains on the calibrated coefficients. We chose to use a discharge-independent value of 38 $m^{1/2} s^{-1}$ for the Chézy coefficient in the floodplains, since the variations of this coefficient are small in the calibration (Figure 9).

To analyse the performance of the extended SOBEK model presented in this paper, computed water levels are compared to the results of the originally calibrated model in which the roughness coefficients are a function of the discharge (Figure 8). Figure 10 shows stage–discharge relationships for steady flow and for the two flood waves as computed with the SOBEK model, using calibrated roughness coefficients as a function of discharge (Figure 9). In the steady calculation, for each discharge the SOBEK model iterates water levels along the 60 km reach until steady flow conditions are obtained, yielding a stage–discharge relationship without hysteresis. For the unsteady calculations however, the effect of accelerations and decelerations due to the passage of a non-uniform flood wave (i.e. the water surface slope is different from the average channel slope) is included in SOBEK, since the unsteady terms are retained in the equation of motion. Compared to the steady computation, this results in lower water levels during the rising stage (i.e. the wave accelerates) and higher water levels during the falling stage, for both types of flood waves. The maximum water level difference between the rising and falling stage is larger for the broad-peaked flood wave (≃1 m) than for the sharp-peaked flood wave (≃0·7 m). This is because the discharge variations during the rising and falling stage are more gradual for the sharp-peaked flood wave (Figure 7), leading to smaller acceleration and deceleration effects.

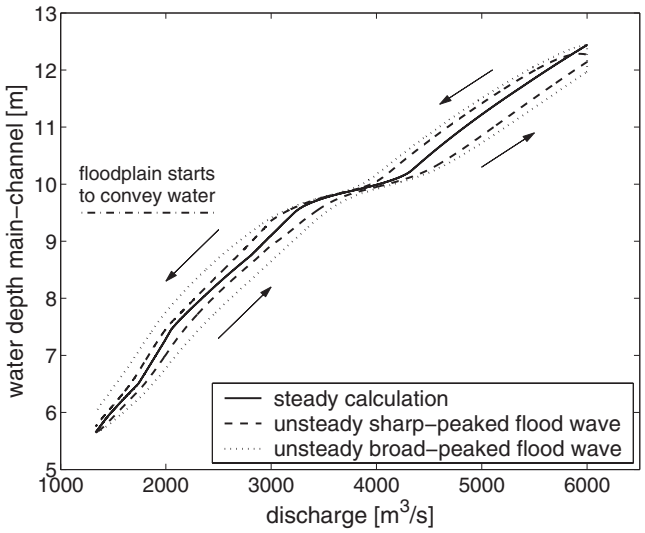

Figure 10. Stage–discharge relationships for a steady and unsteady SOBEK calculation using calibrated roughness coefficients for two types of flood waves (at the upstream model boundary). The arrows indicate the direction of the hysteresis.

Results of the Extended Sobek Model

Dune dynamics for sharp-peaked flood wave

Figure 11 shows simulated dune dynamics for the case with a sharp-peaked flood wave, with constant dune length and with variable dune length. For constant dune length, the simulated dune height reaches a value of about 2 m (Figure 11b). Wilbers and Ten Brinke (2003) report dune heights of ~1–1·2 m for a reach in the River Waal at peak discharge, for a dune length of 40 m. Thus our simulations compare quite well with measured dimensions, if we take into account that the dune evolution model predicts maximum dune dimensions rather than average dune dimensions (accounts for a factor 2 difference; see section 'Roughness model'). Simulations show small variations in dune height due to discharge variations (Figure 11b), and the maximum dune height occurs about 3 days after the peak discharge, which is comparable to measurements in the River Rhine (Wilbers and Ten Brinke, 2003). The hysteresis effects will be discussed below in more detail. For a variable dune length, the model predicts increasing dune lengths during the rising stage due to an increasing water depth in the main channel (Figure 11a). Elongating dunes have smaller bed slopes and grains can be transported upslope more easily, resulting in higher dunes (Figure 11b). As a result, the dune height becomes up to 40% higher than for a constant dune length.

If the dune length is constant, a more or less constant aspect ratio of about 0·055 is obtained (Figure 11c). For variable dune length, the simulated dune aspect ratio varies between 0·05 and 0·07 (Figure 11c), which is well within the range of values from the literature (e.g. Bennett and Best, 1995; McLean *et al*., 1999; Carling *et al*., 2000). In the River Rhine, also lower values around 0·04 are reported (Julien and Klaassen, 1995; Wilbers and Ten Brinke, 2003). As discussed in section 'Roughness model', the dune height may be over-predicted for natural river settings which may explain the slightly higher dune aspect ratios. At the second discharge peak, the dune height is higher than at low discharge (Figure 11b), while the dune aspect ratio is lowest at the peak discharge (Figure 11c). This is because the dune length is largest at the peak discharge and differs by ~100% between low and high discharge, while the dune height differs by ~40% between low and high discharge (Figure 11). Since the dune aspect ratio is important for roughness predictions (Equation (3)), a proper modelling of this aspect ratio is very important for accurate modelling of dynamic roughness due to dunes.

Figure 11d shows that the migration rate is highly variable and especially responds to a changing discharge. This is not surprising, since for increasing discharge and flow depth the bed shear stress and thus the sediment transport increase. For constant dune length, the dune height becomes more or less constant in time, while the migration rate still varies significantly (Figure 11d). Apparently, the flow depth (or bed shear stress) is the controlling parameter on the migration rate in the case of constant dune length. Wilbers and Ten Brinke (2003) assumed a relationship between dune length and migration rate with higher migration rates for longer dunes. If the dune length varies during the flood wave we find similar behaviour (Figures 11a and 11d). However, the relationship is less strong than Wilbers and Ten Brinke (2003) assumed, since longer dunes are also higher, reducing the migration rate if we assume that all sediment that passes the dune crest deposits evenly at the bedform lee (as is done in the dune evolution model).

Hysteresis effect in dune height

Figures 12a and 12b show the dune height as a function of the discharge for constant dune length for the two different flood waves. The maximum dune height is about 2·25 m and the dune height varies by roughly 10 cm between the rising and the falling limbs of the flood waves. For the broad-peaked flood wave, the period of high discharge is relatively long, meaning that the dune height reaches the equilibrium dune height for the prevailing flow conditions. The difference in hysteresis for the two flood waves is due to the difference in rate of change of discharge with time. For the broad-peaked flood wave the rate of change is large and the dune height does not significantly respond to the falling discharge (Figure 12b), while for the sharp-peaked flood wave the dune height variation does respond to the changing discharge (Figure 12a).

For variable dune length, the hysteresis effects in dune height are more pronounced for both flood wave shapes (Figures 12c and 12d) compared to the case with constant dune length. Paarlberg *et al*. (2009) have shown that for equilibrium dunes the dune evolution model predicts a strong correlation between dune length and dune height and that the dune aspect ratio in equilibrium is more or less constant. Since the dune length adapts immediately to changing flow conditions in a simulation with variable dune length (because of the approach used to simulate dune length), also the dune height shows more variation than for the case of a constant dune length.

For the second wave of the sharp-peaked flood wave, we clearly observe a hysteresis loop with a maximum dune height difference of ~1·2 m between the rising and the falling stage. Also, the maximum dune height occurs if the discharge is already falling. The time lag between maximum dune height and maximum discharge of about 3 days (Figure 11b) is caused by the relatively low rate of change in discharge causing the dunes to be still adapting to an equilibrium dune height which is larger than the actual dune height. For the broad-peaked flood wave, the dunes remain somewhat lower during the rising stage of the second wave than is the case for the sharp-peaked flood wave (i.e. ~10 cm; Figures 12c and 12d) because of the larger rate of change in discharge with time. The relatively long period of high discharge for the broad-peaked flood wave yields dunes that are ~80 cm higher at the start of the falling stage than for

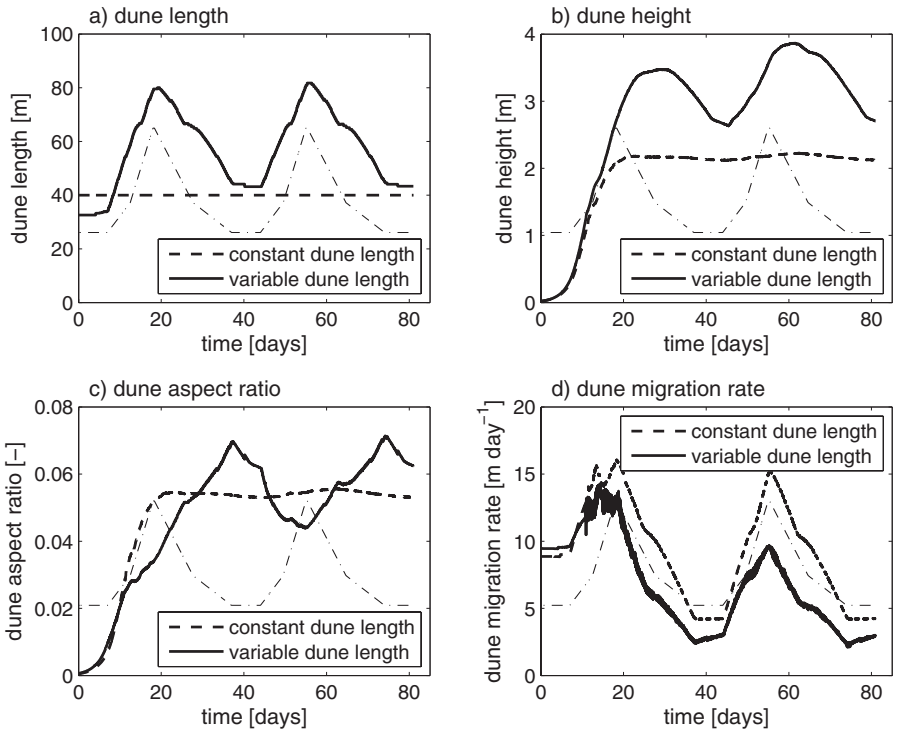

Figure 11. Result for sharp-peaked flood wave (Figure 7a). Dash-dotted lines represent the discharge variation in a simulation: (a) dune length; (b) dune height; (c) dune aspect ratio (ratio of dune height to dune length); (d) dune migration rate.

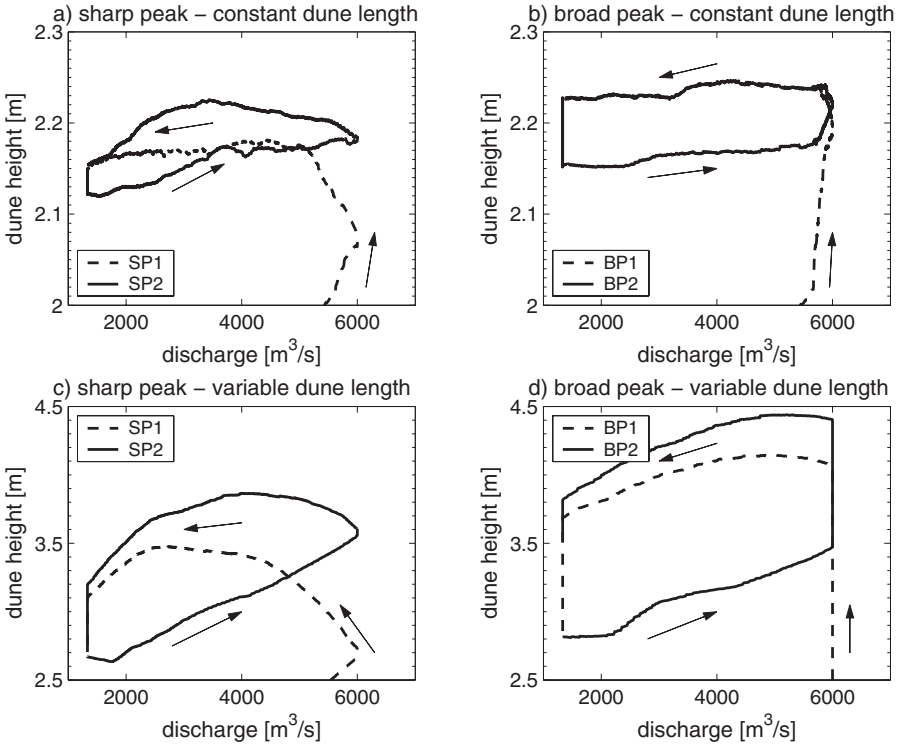

Figure 12. Hysteresis in dune height for the two types of flood waves (Figure 7). Results for both constant dune length (a, b) and variable dune length (c, d) are shown (note different scales on *y*-axis). In the figures, the flood waves (which occur in series) in each simulation are plotted separately (in the legends, 'BP' is broad-peaked and 'SP' is sharp-peaked, while '1' indicates the first and '2' the second wave; Figure 7).

the sharp-peaked flood wave. This implies that at the start of the falling stage the dune height is almost adapted to the new flow conditions (and dune length), meaning that the time lag in dune height during the falling stage is very small and almost negligible. Note that after the floods the simulated dune heights differ between the two types of flood waves. At the end of the flood wave the relict dunes are higher for the broad-peaked flood wave than for the sharp-peaked flood wave. This is important information because these relict dunes may cause problems for navigation, for example, and the dunes may diminish in height slowly at low discharge, because the transport rates are relatively low.

Effects of dune evolution on hydraulics

Changing dune dimensions in time and the hysteresis effect in dune height also yield temporal variations and hysteresis in roughness height, since the roughness coefficient of the main channel is directly linked to both dune height and dune length (Equation (3)). Figure 13 compares Chézy coefficients computed with the new dynamic roughness model and the values of the originally calibrated model (Figure 8). Results are only shown for the second wave in a simulation.

The new dynamic roughness model yields lower Chézy coefficients (higher roughness), for both types of flood waves,

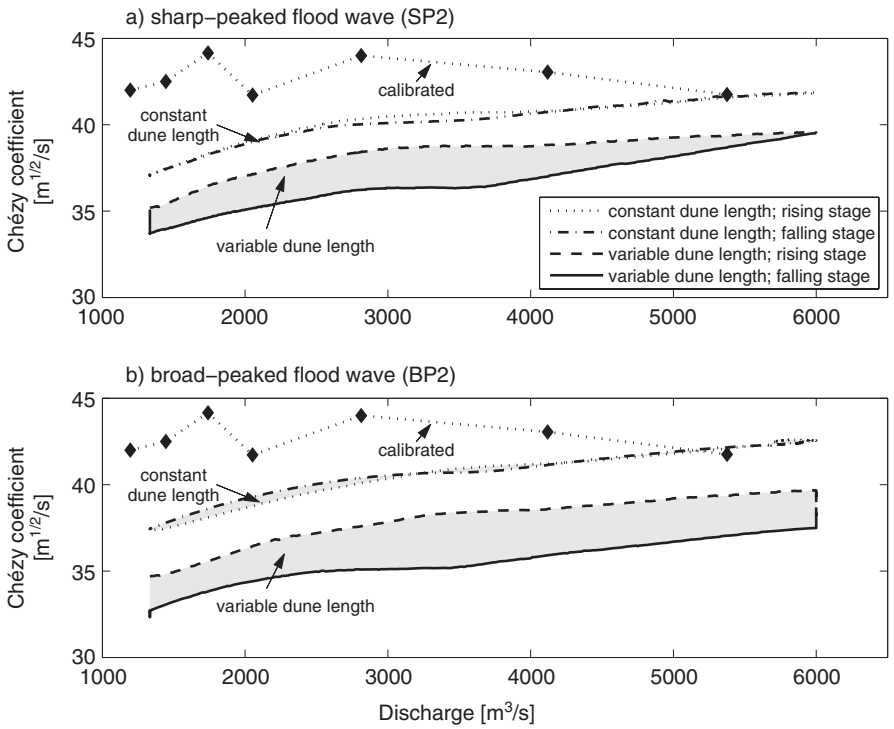

Figure 13. Chézy coefficients of the main channel computed by the dynamic roughness model, compared to the calibrated values (diamond symbols) for (a) sharp-peaked flood wave and (b) broad-peaked flood wave. Results for both constant and variable dune length are shown, for the second flood wave of a simulation (Figure 7).

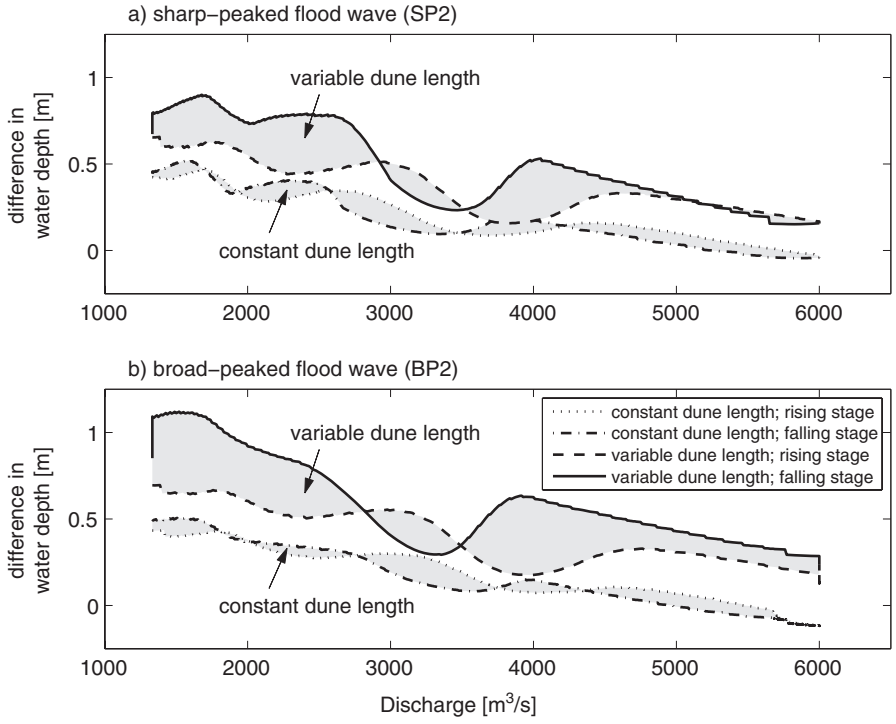

Figure 14. Differences in the stage–discharge relationships between the SOBEK model extended with a dynamic roughness model and the originally calibrated SOBEK model (Figure 8) for (a) sharp-peaked flood wave and (b) broad-peaked flood wave Results for both constant and variable dune length are shown, for the second flood wave of a simulation (Figure 7).

especially in the case of variable dune length, which is directly linked to the higher dunes for these cases (Figure 12). For constant dune length, the roughness coefficient at the peak discharge is predicted quite well. The hysteresis effect in roughness is very small for constant dune length, which is due to the dune height being almost constant during the second discharge peak (Figures 12a and 12b). On the other hand, for variable dune length, the Chézy coefficient is 5–10% lower (higher roughness) during the falling stage, compared to the rising stage. Furthermore, this effect is larger for the broad-peaked flood wave, with even lower Chézy coefficients in the early phase of the falling stage (i.e. when the discharge is still high), than during the falling stage of the sharp-peaked flood wave. This illustrates the dependence of roughness predictions on the shape of a flood wave. The differences between the new dynamic roughness model and the originally calibrated roughness coefficients are largest at low discharge. At low discharge, Chézy coefficients are about 13% lower for the constant dune length and about 22% for the variable dune length.

Figure 14 shows the difference between the water levels computed with the dynamic roughness model and the original stage–discharge relationship for both flood wave types (using the method presented in Figure 8). Since the time evolution of the main channel roughness differs between the dynamic roughness model and the calibrated model, water levels are different for a certain discharge. This implies that certain areas become flooded or dry at different discharges. This is the reason for the oscillations in Figure 14.

Table I. Sensitivity analysis for roughness correction factor γ for sharp-peaked flood wave and variable dune length. C_m is the main channel Chézy coefficient, and h_{diff} represents the difference in flow depth between the extended SOBEK model and the SOBEK model adopting calibrated roughness coefficients. The overbar indicates that a certain parameter is averaged over the second flood wave of a simulation (SP2 in Figure 7).

Case	γ	Δ_{max} (m)	$\overline{\Delta}$ (m)	$\overline{\lambda}$ (m)	$\overline{(\Delta/\lambda)}$	$\overline{C_m}$ ($m^{1/2}$ s^{-1}]	$\overline{h_{diff}}$ (m)
Calibrated model						42·7	
γ −50%	0·175	3·72	3·15	57·5	0·055	41·7	0·09
γ reference	0·35	3·86	3·32	60·3	0·055	36·6	0·53
γ +50%	0·525	3·96	3·42	62·2	0·055	33·5	0·82

Generally, water levels are higher using the new dynamic roughness model, as a result of lower Chézy coefficients. The differences are largest at low discharge, if most water is conveyed through the main channel, and smallest at peak discharge. This is attributed to the aspects that (i) in practice hydraulic models are calibrated on peak discharges and (ii) the relative influence of the main channel roughness decreases at higher water levels. Dunes reach their maximum dimensions after the peak discharge (Figure 12) and decrease in dimensions slowly after they have reached their maximum dimensions. Therefore, for variable dune length, differences in flow depth are larger for the falling stage than for the rising stages. Differences in water depth can be up to 1 m for low discharge (Figure 14), which is a difference in water depth of ~15% between the new dynamic roughness model and a SOBEK model adopting calibrated roughness coefficients. For the broad-peaked flood wave, effects are even larger than for the sharp-peaked flood wave, since dunes are higher for that case.

Discussion

Dune evolution model

In rivers, dune fields often show three-dimensional (3-D) structures, such as amplitude variations or crestline curvature (e.g. Allen, 1968; Best, 2005, and references therein). Another 3-D phenomenon is that dunes do not necessarily cover the full main channel width, due to lateral grain-size differences, horizontal flow patterns and sediment diffusion processes. The dune evolution model does not take lateral variations in dune dimensions into account, since it is a 2-D vertical (2-DV) model. Although 3-D dune shapes are observed in nature, the general pattern of dune formation is often aligned with the main flow direction (e.g. Figure 1c), if the river is not too wide (generally, 3-D bed features are observed for width to depth ratios larger than 3 (Crickmore, 1970; Williams, 1970)). Thus, if a river is relatively narrow and the flow is confined between groynes aligning the flow more or less in one direction, a 2-DV dune evolution model is thought to be representative.

In section 'Roughness model', it is argued that computed dune dimensions represent maximum dune heights rather than average dune heights, giving rise to adaptation of the roughness correction factor γ. However, this over-prediction could also be caused by physical processes that are currently not captured by the dune evolution model (see also Paarlberg, 2008; Paarlberg *et al*., 2009), such as suspended sediment transport, non-uniform sediment dynamics, or the aspect that part of the bed load transport passes the separation point, effectively not contributing to dune formation. These aspects remain for future research.

Dune roughness model

Observations show that dune fields are characterized by bedforms of different spatial scales (e.g. Julien *et al*., 2002; Wilbers and Ten Brinke, 2003; Jerolmack and Mohrig, 2005). During unsteady flow events in the River Rhine, it is observed that during the falling stage of a flood wave secondary dunes form on the primary dunes, because the primary dunes cannot instantaneously adapt to the changing flow conditions (Wilbers and Ten Brinke, 2003). According to Wilbers (2004) it is important to distinguish between primary and secondary dunes for roughness predictions. Additionally, Schindler and Robert (2005) and Fernandez *et al*. (2006) showed that the effects of amalgating dunes of different scales on turbulence structures in the flow field, also influence the total flow resistance caused by dunes. This behaviour cannot be captured by the dynamic roughness model, since there is no mechanism present that allows for the formation of these secondary dunes. Knowledge on the exact influence of secondary dunes on flow resistance is still limited (Best, 2005). Numerical simulations of the turbulent flow over trains of irregular bedforms could give insight into the controlling dune dimensions on the total flow resistance. In the dynamic roughness model, during the falling stage of a flood wave the water depth and dune length decrease. In reality this reduction in dune length manifests via the formation of secondary dunes, while in the dune evolution model the domain length is shortened, also leading to shorter (and lower) dunes.

This paper shows that hysteresis effects in dune height yield significant differences in roughness coefficients between the rising and falling stages. These hysteresis effects are not included in the model using calibrated roughness coefficients. This explains part of the differences in Chézy coefficients and water levels between the new dynamic roughness model and the model using calibrated Chézy coefficients.

In the dune roughness model a roughness correction coefficient $\gamma = 0{\cdot}35$ is introduced into Equation (3) to correct for the effects of the shape of the dune lee face and plan form and a translation to representative average dune dimensions (see section 'Roughness model'). A sensitivity analysis shows that varying this parameter has marginal influence on dune characteristics (Table 1). However, the influence on Chézy coefficients and water depths is significant, since the Nikuradse roughness height of the main channel linearly depends on γ. Effectively, the stage–discharge relationships shift upwards or downwards depending on γ. Apparently, changes in roughness coefficients and water depths do not change the flow significantly, leading to similar dune characteristics. The effect of this correction indicates that future research is required on the relationship between dune dimensions and plan form of dunes on roughness coefficients.

Model application to different river systems

The dynamic roughness model presented in this paper is built around the hydraulic simulation model SOBEK, which includes the effects of floodplains, groynes and variable streamwise cross-sectional shapes, for example. This allows representation of natural river configurations with the model,

since realistic parameters of the main channel can be used to determine dune evolution. In turn, dune evolution in the main channel influences the flow over the entire cross-section since the roughness coefficient of the main channel changes.

This paper discusses model application to a branch of the River Rhine which is a mildly sloping sand-bed river with generally low Froude numbers, i.e. 0·1–0·35 (Van Vuren *et al*., 2005). Therefore, the model approach can also be applied to similar river systems such as the Mississippi River in the USA or the Paráná River in Argentina. It should be noted that the applied flood wave shapes as used in this paper are based on data from the River Rhine. The sharp-peaked flood wave used in the present paper might not be 'sharp' at all in other river systems. The flood wave shape, however, can easily be changed to study the effect of different flood wave shapes.

Also in estuarine systems, dune-like features are observed (e.g. Kostaschuk, 2000; Kostaschuk and Best, 2004; Francken *et al*., 2004; Villard and Church, 2005). Estuarine dunes are often quite symmetrically shaped, due to the oscillatory tidal flow in estuarine environments. However, the degree of symmetry depends on the relative flow strength in each direction. If one of the directions is dominant, then the estuarine dunes might develop an angle-of-repose leeside like dunes in a unidirectional flow. In such cases, the dune evolution model used in this paper can be applied; however, a problem occurs if the flow reverses, and the estuarine dune still has an angle-of-repose leeside that becomes exposed to the flow. To apply the model in this case, we need a description of the roughness of this leeside that blocks the flow and some model for the morphological adaptation of the leeside.

Grain-size sorting within bedforms influences dune formation and the grains present on the surface of dunes (e.g. Miwa *et al*., 2001; Blom *et al*., 2003; Kleinhans, 2004). Miwa *et al*. (2001) argue that the presence of relatively coarse sediment restrains the development and growth of bedforms, while fine sediment promotes bedform growth and collapse of bedforms. Effectively, this may lead to more irregular bedform patterns than considering uniform sediment. In the dune evolution model, the sediment transport rate is based on the median grain diameter, i.e. the D_{50} of the sediment, and the bed material is assumed to be uniform. Paarlberg *et al*. (2009) have shown that a different grain size does not influence equilibrium dune dimensions, although it does influence timescales to equilibrium, which is important in the dynamic roughness model.

Practical implications of the model results

The new dynamic roughness model provides insight into the part of the main channel roughness coefficient associated with time-dependent dune evolution and hysteresis effects of dunes. The model is computationally efficient: typically, two flood waves in series, e.g. Figure 7a with a duration of 80 days, take about 8 hours to compute on a standard office PC.

Dune dynamics and associated hysteresis effects can be excluded from calibrated roughness coefficients by using the dynamic roughness model of this thesis. In practice, however, model calibration will still be required, because of other uncertainties originating from errors in the hydraulic model itself or errors in the model schematization. This aspect could be included in model calibration by rewriting Equation (2) as

$$k_m = k_{grains} + k_{dunes} + k_{uncertain} \quad (4)$$

in which the term $k_{uncertain}$ represents uncertainties and model errors contributing to the roughness coefficient of the main channel. This term is not taken into account for the comparisons made in this paper, since it is not known for the SOBEK model that uses calibrated roughness coefficients. It is likely that the water-level measurements that were used in the original SOBEK calibration included effects due to dunes, but to what extent is not known. A starting point for future model calibrations should be to use the dynamic roughness model presented in this paper to predict the main channel roughness, and calibrate the term $k_{uncertain}$ in Equation (4) or other model parameters to take model uncertainties into account. Preferably, simultaneous dune and water-level measurements should be available for this calibration.

In nature, flood waves often come in series, meaning that relict dunes might still be present if the discharge increases again at the start of a new flood wave. Because the models presented in this paper require minimal computational effort, a series of flood waves of various shape can be simulated to investigate the role of this history effect. Model results clearly show that computed dune dimensions are different between the first and second flood wave in a simulation (Figures 11 and 12). This also results in differences in roughness coefficients and water depths for the two waves. The hysteresis effects in dune height and associated effects on water depths were analysed for the second flood wave, i.e. for a situation in which the dunes were almost in equilibrium with flow conditions at the start of the wave. Keeping this in mind, the differences between the new dynamic roughness model and the SOBEK model that adopts calibrated roughness coefficients would probably be smaller due to smaller dune heights for the first flood wave. This illustrates the importance of having simultaneous measurements of water levels and dune dimensions during floods, which could improve model calibrations.

Conclusions

This paper presents an extension of the existing hydraulic simulation model SOBEK to a 'dynamic roughness model', in which time-dependent dune evolution is included to explicitly take into account drag due to dunes. The dynamic roughness model consists of a process-based dune evolution model and the roughness predictor of Van Rijn (1984). By computing dune dimensions during a flood wave, the main channel roughness coefficient in SOBEK is dynamically changed and hysteresis effects attributed to dune evolution are taken into account.

Model application to two types of flood waves (i.e. a sharp-peaked and a broad-peaked flood wave) shows significant deviations from calibrated roughness coefficients due to dune evolution during floods. Model results show that differences in the rate of change of discharge with time for the sharp-peaked and the broad-peaked flood wave affect predicted dune dimensions. Also, the relatively long duration of the maximum discharge for the broad-peaked flood wave is important, since dunes can grow further in height during this period. For variable dune length, the Chézy coefficient is 5–10% lower during the falling stage compared to the rising stage. This emphasizes the dependence of roughness predictions on the shape of the flood wave, a factor that is not taken into account if hydraulic simulation models are calibrated on recorded water levels. In the new dynamic roughness model of this paper this dependency is automatically taken into account, since dune dynamics are explicitly simulated.

At low discharge, Chézy coefficients in the dynamic roughness model are 13–22% lower (higher roughness) compared to the SOBEK model using calibrated Chézy coefficients. Furthermore, the hysteresis effect in dune height and dune roughness

cause the water depths to vary significantly between the rising and the falling stages of a flood wave. Both types of flood wave (and variable dune length) lead to an increase in water depth of up to 1 m compared to a case with calibrated roughness coefficients.

The predicted water levels are sensitive to the value of the roughness correction factor γ, which is a rather uncertain parameter in the dynamic roughness model and might even depend on dune plan form. Therefore future research should focus primarily on the part of the new dynamic roughness model that translates computed dune dimensions into a roughness coefficient. Although calibration of roughness coefficients of hydraulic models will remain necessary, the effects of dune dynamics can be excluded from the calibration using the modelling approach presented in this paper.

Acknowledgements—This research is supported by the Technology Foundation STW, Applied Science Division of NWO and the Technology Program of the Ministry of Economic Affairs (Project No. 06222). We would like to thank the organizing committee of the MARID conference to arrange for this special issue. Also, the reviewers are acknowledged for their suggestions to improve this paper.

References

Allen JRL. 1968. *Current Ripples: Their Relation to Patterns of Water and Sediment Motion*. North-Holland: Amsterdam.

Allen JRL. 1976. Computational models for dune time-lag: general ideas, difficulties and early results. *Sedimentary Geology* **15**: 1–53.

ASCE Task Force on Friction Factors in Open Channels. 1963. Friction factors in open channels. *Journal of Hydraulic Engineering* **89**(HY2): 97–143.

Bennett SJ, Best JL. 1995. Mean flow and turbulence structure over fixed, two dimensional dunes: implications for sediment transport and bedform stability. *Sedimentology* **42**(3): 491–513.

Best J. 2005. The fluid dynamics of river dunes: a review and some future research directions. *Journal of Geophysical Research* **110**: F04S01.

Blom A, Ribberink JS, de Vriend HJ. 2003. Vertical sorting in bed forms: flume experiments with a natural and a trimodal sediment mixture. *Water Resources Research* **39**(2): 1025.

Carling PA, Gölz E, Orr HG, Radecki-Pawlik A. 2000. The morphodynamics of fluvial sand dunes in the River Rhine, near Mainz, Germany. I. Sedimentology and morphology. *Sedimentology* **47**: 227–252.

Casas A, Benito G, Thorndycraft VR, Rico M. 2006. The topographic data source of digital terrain models as a key element in the accuracy of hydraulic flood modelling. *Earth Surface Processes and Landforms* **31**: 444–456.

Coleman SE, Zhang MH, Clunie TM. 2005. Sediment-wave development in subcritical water flow. *Journal of Hydraulic Engineering* **131**(2): 106–111.

Crickmore MJ. 1970. Effects of flume width on bed form characteristics. *Journal of the Hydraulics Division, ASCE* **96**(HY2, paper 7077): 473–496.

De Vriend HJ. 2006. Flood management research needs. In *Floods, from Defence to Management: Third International Symposium on Flood Defence*, Van Alphen J, Van Beek E, Taal M (eds); 49–61.

Dodd N, Blondeaux P, Calvete D, de Swart HE, Falques A, Hulscher SJMH, Rozynski G, Vittori G. 2003. Understanding coastal morphodynamics using stability methods. *Journal of Coastal Research* **19**(4): 849–865.

Fernandez R, Best J, López F. 2006. Mean flow, turbulence structure, and bed form superimposition across the ripple–dune transition. *Water Resources Research* **42**: W05406.

Francken F, Wartel S, Parker R, Taverniers E. 2004. Factors influencing subaqueous dunes in the Scheldt Estuary. *Geo-Marine Letters* **24**(1): 14–21.

Giri S, Yamaguchi S, Shimizu Y, Nelson J. 2007. Simulating temporal response of bedform characteristics to varying flows. In *Proceedings of the 5th IAHR symposium on River, Coastal and Estuarine Morphodynamics*, Vol. 2, Enschede, Netherlands, Dohmen-Janssen CM, Hulscher SJMH (eds). Taylor & Francis: London; 939–947.

Jansen PPh, van Bendegom L, van den Berg J, de Vries M, Zanen A. 1979. *Principles of River Engineering: The Non-tidal Alluvial River*. Delftse Uitgevers Maatschappij: Delft, Netherlands.

Jerolmack DJ, Mohrig DC. 2005. A unified model for subaqueous bed form dynamics. *Water Resources Research* **41**: W12421.

Julien PY, Klaassen GJ. 1995. Sand-dune geometry of large rivers during floods. *Journal of Hydraulic Engineering* **121**(9): 657–663.

Julien PY, Klaassen GJ, Ten Brinke WBM, Wilbers AWE. 2002. Case study: bed resistance of Rhine River during 1998 flood. *Journal of Hydraulic Engineering* **128**(12): 1042–1050.

Karim F. 1995. Bed configuration and hydraulic resistance in alluvial-channel flows. *Journal of Hydraulic Engineering* **121**(1): 15–25.

Kleinhans MG. 2004. Sorting in grain flow at the lee side of dunes. *Earth-Science Reviews* **65**: 75–102.

Kleinhans MG, Wilbers AWE, Ten Brinke WBM. 2007. Opposite hysteresis of sand and gravel transport upstream and downstream of a bifurcation during a flood in the River Rhine, the Netherlands. *Netherlands Journal of Geosciences – Geologie en Mijnbouw* **86**(3): 273–285.

Knighton D. 1998. *Fluvial Forms and Processes*. Arnold: London.

Kostaschuk R. 2000. A field study of turbulence and sediment dynamics over subaqueous dunes with flow separation. *Sedimentology* **47**: 519–531.

Kostaschuk R, Best J. 2004. The response of sand dunes to variations in tidal flow and sediment transport: Fraser Estuary, Canada. In *Proceedings of the 2nd international workshop on Marine Sandwave and River Dune Dynamics*, Hulscher SJMH, Garlan T, Idier D (eds), University of Twente and SHOM, Enschede, Netherlands, 1–2 April 2004: 849–863.

McLean SR, Wolfe SR, Nelson JM. 1999. Spatially averaged flow over a wavy boundary revisited. *Journal of Geophysical Research* **104**(C7): 15743–15753.

Miwa H, Daido A, Kato I. 2001. Sand wave transformation with sediment sorting. In *Proceedings of the 8th International Symposium on River Sedimentation*, Cairo, Egypt.

Morvan H, Knight D, Wright N, Tang X, Crossley A. 2008. The concept of roughness in fluvial hydraulics and its formulation in 1D, 2D and 3D numerical simulation models. *Journal of Hydraulic Research* **46**(2): 191–208.

Németh AA, Hulscher SJMH, van Damme RMJ. 2006. Simulating offshore sand waves. *Coastal Engineering* **53**: 265–275.

Ogink HJM. 1988. Hydraulic roughness of bedforms. Report M2017, Delft Hydraulics Laboratory, Delft, Netherlands.

Paarlberg AJ. 2007. Modelnauwkeurigheid en -onzekerheden van in Nederland toegepaste hydraulische modellen: Verslag van interviews met waterbeheerders en modelexperts (in Dutch). Civil Engineering and Management research report 2007R-001/WEM-001, University of Twente, Enschede, Netherlands.

Paarlberg AJ. 2008. Modelling dune evolution and dynamic roughness in rivers. PhD thesis, University of Twente, Enschede, Netherlands.

Paarlberg AJ, Dohmen-Janssen CM, Hulscher SJMH, Termes P. 2007. A parameterization of flow separation over subaqueous dunes. *Water Resources Research*, **43**: W12417.

Paarlberg AJ, Dohmen-Janssen CM, Hulscher SJMH, Termes P. 2009. Modelling river dune evolution using a parameterization of flow separation. *Journal of Geophysical Research*, **114**: F01014.

Perumal M, Shrestha KB, Chaube UC. 2004. Reproduction of hysteresis in rating curves. *Journal of Hydraulic Engineering* **130**(9): 870–878.

Schindler RJ, Robert A. 2005. Flow and turbulence structure across the ripple–dune transition: an experiment under mobile bed conditions. *Sedimentology* **52**: 627–649.

Sieben J. 2003. Estimation of effective hydraulic roughness in non-uniform flow. In *Proceedings of the 30th IAHR Congress*, Vol. II, Theme C, Ganoulis J, Prinos P (eds), Thessaloniki, Greece; 17–24.

Termes APP. 2004. Herziening Qh-relaties Venlo en Megen en afleiding Qh-relaties Belfeld-beneden en Lith-boven. Technical Report PR902 (in Dutch), HKV Consultants, Lelystad, Netherlands.

Udo J, Bakker M, Termes P. 2007. SOBEK-model Rijn: hydraulische calibratie. Report PR1158 (in Dutch), HKV Consultants, Lelystad, Netherlands.

Van den Brink NGM, Beyer D, Scholten MJM, van Velzen EH. 2006. Onderbouwing hydraulische randvoorwaarden 2001 van de Rijn en zijn takken. RIZA report 2002·015 (in Dutch), RIZA, Netherlands.

Van der Klis H. 2003. Uncertainty analysis applied to numerical models of river bed morphology. PhD thesis, University of Delft, Netherlands.

Van der Mark CF, Blom A, Hulscher SJMH. 2007. Variability in bedform characteristics using flume and river data. In *Proceedings of the 5th IAHR symposium on River, Coastal and Estuarine Morphodynamics*, Vol. 2, Dohmen-Janssen CM, Hulscher SJMH (eds). Enschede, Netherlands. Taylor & Francis: London; 923–930.

Van Rijn LC. 1984. Sediment transport. Part III: Bed forms and alluvial roughness. *Journal of Hydraulic Engineering* **110**(12): 1733–1754.

Van Rijn LC. 1993. *Principles of Sediment Transport in Rivers, Estuaries and Coastal Seas*. AQUA: Amsterdam.

Van Vuren S, de Vriend HJ, Ouwekerk S, Kok M. 2005. Stochastic modelling of the impact of flood protection measures along the River Waal in the Netherlands. *Natural Hazards* **36**: 81–102.

Vanoni VA, Hwang LS. 1967. Relation between bed forms and friction in streams. *Journal of the Hydraulic Division, ASCE* **93**: 121–144.

Vidal J-P, Moisan S, Faure J-B, Dartus D. 2007. River model calibration, from guidelines to operational support tools. *Environmental Modelling and Software* **22**: 1628–1640.

Villard PV, Church M. 2005. Bar and dune development during a freshet: Fraser River Estuary, British Columbia, Canada. *Sedimentology* **52**: 737–756.

Warmink JJ, Booij MJ, van der Klis H, Hulscher SJMH. 2007. Uncertainty in water level predictions due to various calibrations. In *Proceedings of CAIWA 2007*, Pahl-Wostl C (ed.), Basel, Switzerland, 12–15 November 2007; 1–18.

Wasantha Lal AM. 1995. Calibration of riverbed roughness. *Journal of Hydraulic Engineering* **121**(9): 664–671.

Werner M. 2004. Spatial flood extent modelling: a performance-based comparison. PhD thesis, Delft University of Technology, Netherlands.

Wilbers AWE. 2004. The development and hydraulic roughness of subaqueous dunes. PhD thesis, University of Utrecht, Netherlands.

Wilbers AWE, Ten Brinke WBM. 2003. The response of subaqueous dunes to floods in sand and gravel bed reaches of the Dutch Rhine. *Sedimentology* **50**: 1013–1034.

Williams PG. 1970. Flume width and water depth effects in sediment transport experiments. Geological survey professional paper 562-H, US Department of the Interior, Washington, DC.

Yalin MS. 1964. Geometrical properties of sand waves. *Journal of the Hydraulics Division, ASCE* **90**(5): 105–119.

Yalin MS. 1972. *Mechanics of Sediment Transport*. Pergamon Press: New York.

